Fig. 1

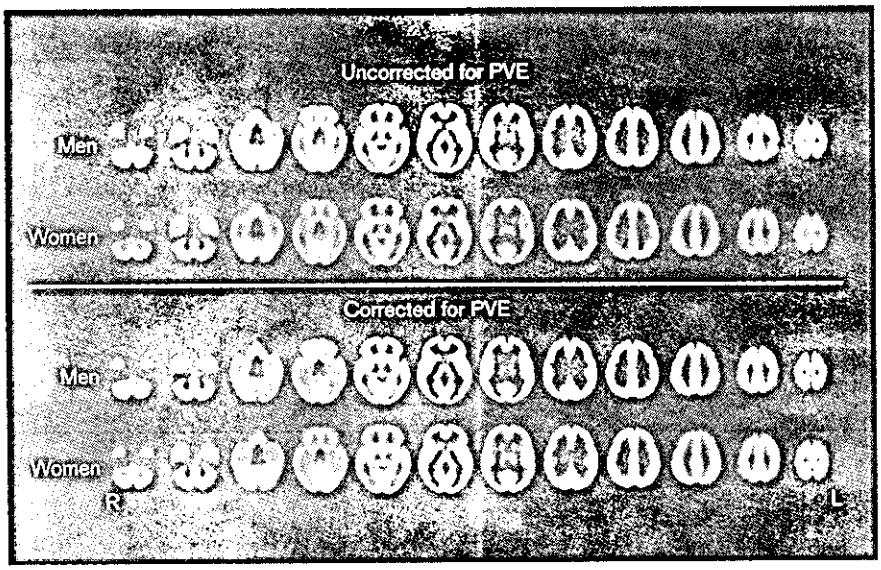

Spatially normalized SPECT images, as an average, in 20 healthy men and 20 healthy women before and after correction for partial volume effects (PVEs). Note the more homogenous distribution of regional cerebral blood flow (rCBF) after PVE correction.

Fig. 2

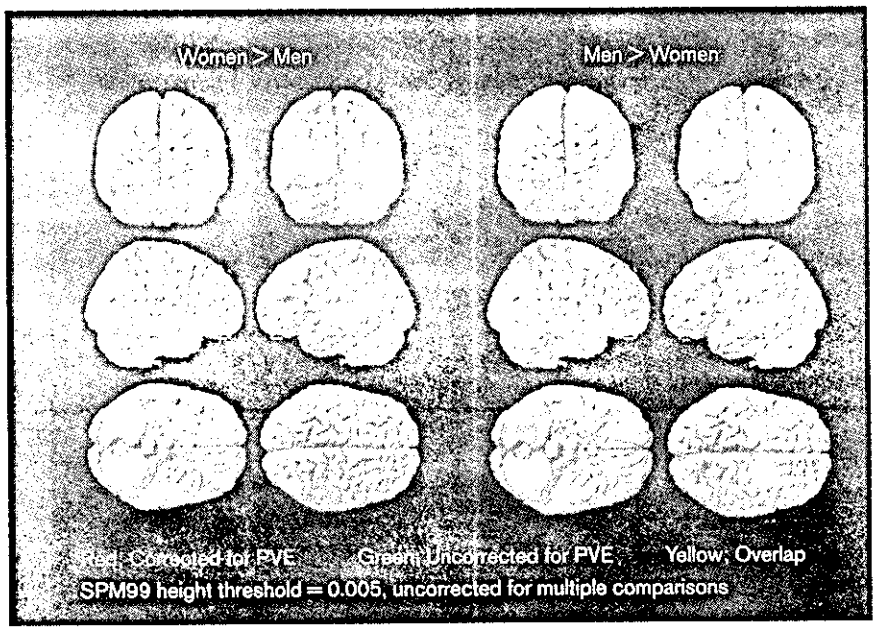

SPM99 results for differences of adjusted rCBF between healthy men and women before and after PVE correction. Dual colour display on surface rendered images of the standard MRI scans of significant gender differences (height threshold $P<0.005$, uncorrected for multiple comparisons) of adjusted rCBF before correction of PVEs as green and those of adjusted rCBF after PVE correction as red in aged healthy volunteers by SPM99. Overlapping areas are shown as yellow. (Abbreviations as in the legend to Fig. 1).

part of the left superior temporal gyrus and left supramarginal gyrus. This may result from increased grey matter volume in the left superior temporal gyrus in women as shown in Fig. 3.

Another consistent finding in gender differences in behaviours is that men excel in certain visuospatial tasks [1]. In the present study, PVE correction revealed that men had higher adjusted rCBF in right parietal lobes and

Table 1 Gender differences in brain perfusion SPECT before and after PVE correction

SPECT	Region	Brodmann area	Talairach coordinate			*Z* score
			x	*y*	*z*	
SPECT uncorrected for PVE						
Women > men	Left superior temporal gyrus	22	−44	−55	18	4.03
	Left superior temporal gyrus	21	−57	−10	−1	3.16
	Left supramarginal gyurs	39	−44	−55	32	3.08
Men > women	Right medial frontal gyrus	6	14	5	57	4
	Left middle frontal gyrus	6	−28	−7	54	3.81
	Right fusiform gyrus	19	24	−82	−13	3.67
	Right middle frontal gyrus	6	28	−1	52	3.56
	Right cerebellum (posterior lobe)		26	−57	−11	3.1
SPECT corrected for PVE						
Women > men	Right middle temporal gyrus	21	51	−1	−20	3.5
	Left inferior frontal gyrus	46	−50	33	9	3.29
	Left superior temporal gyrus	22	−53	2	−3	3.16
	Left middle temporal gyrus	21	−59	−8	−13	3.02
Men > women	Left superior frontal gyrus	6	−28	−8	63	3.97
	Right medial frontal gyrus	6	14	5	57	3.54
	Right superior parietal lobule	7	14	−61	58	3.53
	Right postcentral gyrus	3	30	−32	57	3.43
	Right cerebellum (posterior lobe)		8	−59	−11	3.37
	Right middle frontal gyrus	6	28	1	53	3.23
	Right fusiform gyrus	19	24	−74	−13	3.1
	Right precuneus	7	26	−73	53	3.03

right fusiform gyrus than women. Although, again, we have to be careful about linking rCBF differences at rest to those under activation, the present resting results after PVE correction more closely resembled the activation results in a visuospatial perception test [32] which involved the right parietal cortex and occipitotemporal junction than did results before PVE correction. Jones *et al.* [11] and Van Laere *et al.* [12] reported similar gender differences in adjusted rCBF of parietal lobes except that in their SPECT studies the direction of the differences was reversed, with women having higher resting rCBF in bilateral parietal lobes than men. Premotor and prefrontal cortices into which long association fibres project from the parietal cortex were also activated in a paradigm of visuospatial perception in a PET study [33]. In spite of larger grey matter volume in premotor and prefrontal cortices in men than in women as shown in Fig. 3, rCBF in these areas still remained higher in men than in women after PVE correction.

By using SPECT, Van Laere and Dierckx [13] found that men had relatively higher resting rCBF in the cerebellum than women. When they compared the perfusion with the grey matter volume measured by MRI, such a gender difference in perfusion was considered to be due to a gender difference in cerebellar volume. In contrast, the present study showed a consistent gender difference in the right cerebellum before and after PVE correction. Gur *et al.* [8] similarly found that men had relatively higher resting rCMRglc in bilateral cerebellar hemispheres compared with women. Volkow *et al.* [10] also reported similar significant differences in cerebellar metabolism between women and men, except that in their study the direction of the differences was reversed, with women having higher metabolism in bilateral cerebellar hemispheres, but none of the reports that mentioned gender differences in cerebellum clarified the detailed location in the cerebellum. In the present study, it is clear that only the right posterior cerebellum showed a gender difference before and after PVE correction. Conventionally, cerebellum is considered to be involved in motor function, but non-traditional roles for it in the regulation of autonomic function, behaviour and cognition are also recognized. As for the posterior lobe corresponding to neocerebellum, besides its role in coordinating extremity movement, non-motor functions, including modulation of thought, planning, strategy formation, spatial and temporal parameters, learning, memory and language have been proposed as well [34].

The discordant findings in gender differences in previous studies on PET or SPECT may be partly attributable to the substantial age differences in the groups studied. This may be particularly relevant for our group, since it included only post-menopausal women, and oestrogen has been considered to affect brain function [4,35]. Moreover, various degrees of brain atrophy among aged subjects would obscure true gender difference especially in a SPECT study with poorer resolution compared with PET. We believe that PVE correction is essential for detecting marginal gender differences in SPECT studies.

Finally, we must refer to the study limitations. First, we examined only the resting state and did not incorporate activation procedures. Thus, our conclusions concern topography of the human brain while it is idling, which

Fig. 3

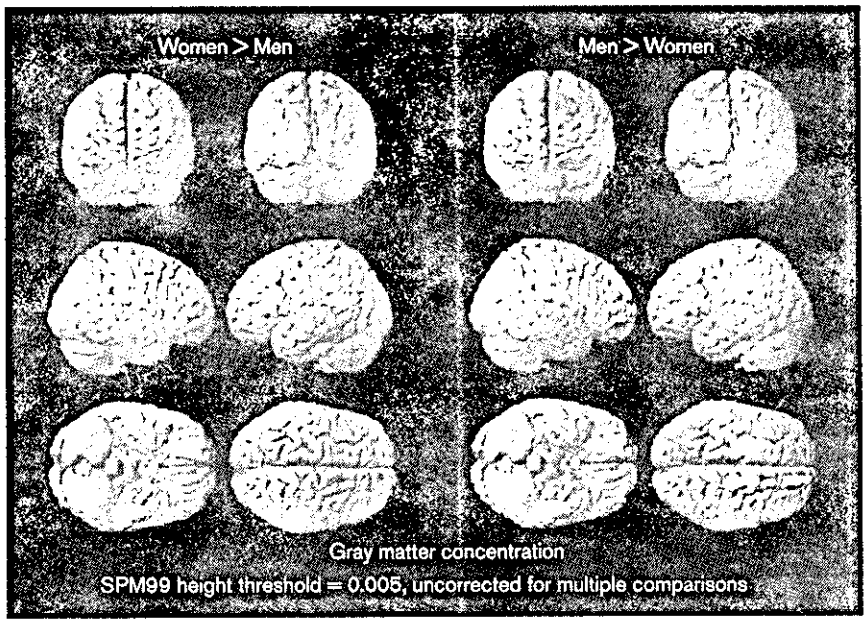

SPM99 results for differences of grey matter volume between healthy men and women. Grey scale display on surface rendered images of the standard MRI scans of significant gender differences (height threshold $P<0.005$, uncorrected for multiple comparisons) of grey matter volume in aged healthy volunteers by SPM99.

Table 2 **Gender differences in grey matter volume**

	Region	Brodmann area	Talairach coordinate			Z score
			x	*y*	*z*	
Women > men	Left superior temporal gyrus	22	−46	−56	16	3.92
Men > women	Right superior frontal gyrus	8	16	47	38	4.30
	Right medial frontal gyrus	10	14	48	−6	3.57
	Left superior frontal gyrus	6	−18	5	55	3.52
	Left medial frontal gyrus	6	−16	−17	56	3.12
	Left precentral gyrus	44	−44	12	12	2.77

may itself influence regional brain activity. Further gender differences may become evident when activity is measured during the performance of behavioural tasks. Nonetheless, measures of resting rCBF support a neurobiological explanation of some gender related differences in behaviour. Second, although the previous phantom study validated the present method for PVE correction, this correction is sensitive to errors, particularly image segmentation and image registration. Therefore we do not totally deny that the differences seen only after PVE correction can be artifacts induced by the correction method than true perfusion differences which were hidden by morphometric variations.

Conclusion

Gender effects on rCBF have not been consistent. Discrepancies among studies probably reflect multiple factors, including study conditions, subjects' characteristics, analysis strategies, and measurement variability. To investigate gender differences in resting rCBF, we focused our attention on correction for PVE in SPECT images of aged healthy women and men. The PVE correction disclosed significant gender differences in rCBF that agreed well with the consistent gender differences in behaviours of better performance noted on verbal tasks in women and on visuospatial tasks in men. Gender differences in grey matter volume agreed less with these gender differences in behaviours than rCBF after PVE correction. This PVE correction may be very helpful in SPECT studies on atrophied brain.

Acknowledgements

We thank the technologists at our hospital for data acquisition and Mr John Gelblum for proofreading this manuscript.

References

1 McGlone J, Kertesz A. Sex differences in cerebral processing of visuospatial tasks. *Cortex* 1973; **9**:313–320.
2 Kimura D, Harsham RA. Sex differences in brain organization for verbal and non-verbal functions. *Prog Brain Res* 1984; **61**:423–441.
3 Ragland JD, Coleman AR, Gur RC, Glanhn DC, Gur RE. Sex differences in brain–behavior relationships between verbal episodic memory and resting regional cerebral blood flow. *Neuropsychologia* 2000; **38**:451–461.
4 Baxter LR, Mazziotta JC, Phelps ME, Selin CE, Guze BH, Fairbanks L. Cerebral glucose metabolic rates in normal human females versus normal males. *Psychiatry Res* 1987; **21**:237–245.
5 Miura SA, Schapiro MB, Grady CL, Kumar A, Salerno JA, Kozachuk WE, *et al.* Effect of gender on glucose utilization rates in healthy humans: a positron emission tomography study. *J Neurosci Res* 1990; **27**:500–504.
6 Azari NP, Rapoport SI, Salerno JA, Grady CL, Gonzalez-Aviles A, Schapiro MB, *et al.* Gender differences in correlations of cerebral glucose metabolic rates in young normal adults. *Brain Res* 1992; **574**:198–208.
7 Andreason PJ, Zametkin AJ, Guo AC, Baldwin P, Cohen RM. Gender-related differences in regional cerebral glucose metabolism in normal volunteers. *Psychiatry Res* 1994; **51**:175–183.
8 Gur RC, Mozley LH, Mozley PD, Resnick SM, Karp JS, Alvai A, *et al.* Sex differences in regional cerebral glucose metabolism during a resting state. *Science* 1995; **267**:528–531.
9 Esposito G, Van Horn JD, Weinberger DR, Berman KF. Gender differences in cerebral blood flow as a function of cognitive state with PET. *J Nucl Med* 1996; **37**:559–564.
10 Volkow ND, Wang GJ, Fowler JS, Hitzemann R, Pappas N, Pascani K, Wong C. Gender differences in cerebellar metabolism: test–retest reproducibility. *Am J Psychiatry* 1997; **154**:119–121.
11 Jones K, Johnson KA, Becker JA, Spiers PA, Albert MS, Holman BL. Use of singular value decomposition to characterize age and gender differences in SPECT cerebral perfusion. *J Nucl Med* 1998; **39**:965–973.
12 Van Laere K, Versijpt J, Audenaert K, Koole M, Goethals I, Achten E, Dierckx R. ^{99m}Tc-ECD brain perfusion SPET: variability, asymmetry and effects of age and gender in healthy adults. *Eur J Nucl Med* 2001; **28**:873–887.
13 Van Laere KJ, Dierckx RA. Brain perfusion SPECT: age- and sex-related effects correlated with voxel-based morphometric findings in healthy adults. *Radiology* 2001; **221**:810–817.
14 Davis SM, Ackerman RH, Correia JA, Alpert NM, Chang J, Buonanno F, *et al.* Cerebral blood flow and cerebrovascular CO_2 reactivity in stroke-age normal controls. *Neurology* 1983; **33**:391–399.
15 Shaw TG, Mortel KF, Meyer JS, Rogers RL, Hardenberg J, Cutaia MM. Cerebral blood flow changes in benign aging and cerebrovascular disease. *Neurology* 1984; **34**:855–862.
16 Devous Sr. MD, Stokely EM, Chehabi HH, Bonte FJ. Normal distribution of regional blood flow measured by dynamic single-photon emission tomography. *J Cereb Blood Flow Metab* 1986; **6**:95–104.
17 Kertesz A, Polk M, Black SE, Howell J. Sex, handedness, and the morphometry of cerebral asymmetries on magnetic resonance imaging. *Brain Res* 1990; **530**:40–48.
18 Gur RC, Gunning-Dixon FM, Turetsky BI, Bilker WB, Gure RE. Brain region and sex differences in age association with brain volume. A quantitative MRI study of healthy young adults. *Am J Geriatr Psychiatry* 2002; **10**:72–80.
19 Mueller-Gaertner HW, Links JM, Prince JL, Bryan RN, McVeigh E, Leal JP, *et al.* Measurement of radiotracer concentration in brain gray matter using positron emission tomography: MRI-based correction for partial volume effects. *J Cereb Blood Flow Metab* 1992; **12**:571–583.
20 Labbe C, Froment JC, Kennedy A, Ashburner J, Cinotti L. Positron emission tomography metabolic data corrected for cortical atrophy using magnetic resonance imaging. *Alzheimer Dis Assoc Disord* 1996; **10**:141–170.
21 Meltzer CC, Zubieta JK, Brandt J, Tune LE, Mayberg HS, Frost JJ. Regional hypometabolism in Alzheimer's disease as measured by positron emission tomography after correction for effects of partial volume averaging. *Neurology* 1996; **47**:454–461.
22 Ibanez V, Pietrini P, Furey ML, Alexander GE, Millet P, Bokde AL, *et al.* Regional glucose metabolic abnormalities are not the result of atrophy in Alzheimer's disease. *Neurology* 1998; **50**:1585–1593.
23 Matsuda H, Kanetaka H, Ohnishi T, Asada T, Imabayashi E, Nakano S, *et al.* Brain SPET abnormalities in Alzheimer's disease before and after atrophy correction. *Eur J Nucl Med* 2002; **29**:1502–1505.
24 Matsuda H, Ohnishi T, Asada T, Li ZJ, Kanetaka H, Imabayashi E, *et al.* Correction for partial-volume effects on brain perfusion SPECT in healthy men. *J Nucl Med* 2003; **44**:1243–1252.
25 Wechsler D. *Wechsler Memory Scale–Revised, Manual.* New York: The Psychological Corporation; 1987. (Japanese edition by Nihon-bunkakagakusha; 2001, pp. 10–57.)
26 Folstein MF, Folstein SE, McHugh PR. Mini-Mental State: a practical method for grading the cognitive state of patients for the clinician. *J Psychiatr Res* 1975; **12**:189–198.
27 Wechsler D. *Wechsler Adult Intelligence Scale–Revised, Manual.* Cleveland, Ohio: The Psychological Corporation; 1981. (Japanese edition by Nihon-bunkakagakusha; 1990, pp. 69–128.)
28 Talairach J, Tournoux P. *Co-planar Stereotaxic Atlas of the Human Brain.* New York, NY: Thieme Medical; 1988, pp. 93–108.
29 Ohnishi T, Matsuda H, Hashimoto T, Kunihiro T, Hishikawa M, Uema T, Sasaki M. Abnormal regional cerebral blood flow in childhood autism. *Brain* 2000; **123**:1838–1844.
30 Ohnishi T, Matsuda H, Tabira T, Asada T, Uno M. Changes in brain morphology in Alzheimer disease and normal aging: Is Alzheimer disease an exaggerated aging process? *Am J Neuroradiol* 2001; **22**: 1680–1685.
31 Audenaert K, Brans B, Van Laere K, Lahorte P, Versijpt, van Heeringen K, Dierckx R. Verbal fluency as a prefrontal activation probe: a validation study using ^{99m}Tc-ECD brain SPET. *Eur J Nucl Med* 2000; **27**: 1800–1808.
32 Faillenot I, Decety J, Jeannerod M. Human brain activity related to the perception of spatial features of objects. *Neuroimage* 1999; **10**: 114–124.
33 Ghatan PH, Hsife JC, Wirsen-Meuriling A, Wredling R, Eriksson L, Stone-Elander S, *et al.* Brain activation induced by the perceptual maze test: A PET study of cognitive performance. *Neuroimage* 1995; **2**:112–124.
34 Afifi AK, Bergman RA. *Functional Neuroanatomy.* New York, NY: McGraw-Hill; 1998, pp. 326–327.
35 Joseph JA, Kochman K, Roth GS. Reduction of motor behavioral deficits in senescence via chronic prolactin or estrogen administration: time course and putative mechanisms of action. *Brain Res* 1989; **505**:195–202.

Superiority of 3-Dimensional Stereotactic Surface Projection Analysis over Visual Inspection in Discrimination of Patients with Very Early Alzheimer's Disease from Controls Using Brain Perfusion SPECT

Etsuko Imabayashi, MD[1,2]; Hiroshi Matsuda, MD[1]; Takashi Asada, MD[3]; Takashi Ohnishi, MD[1]; Shigeki Sakamoto, MD[1]; Seigo Nakano, MD[4]; and Tomio Inoue, MD[2]

[1]Department of Radiology, National Center Hospital for Mental, Nervous, and Muscular Disorders, National Center of Neurology and Psychiatry, Tokyo, Japan; [2]Department of Radiology, Yokohama City University School of Medicine, Yokohama, Japan; [3]Department of Neuropsychiatry, Institute of Clinical Medicine, University of Tsukuba, Ibaraki, Japan; and [4]Department of Geriatric Medicine, National Center Hospital for Mental, Nervous, and Muscular Disorders, National Center of Neurology and Psychiatry, Tokyo, Japan

In Alzheimer's disease (AD), regional cerebral blood flow (rCBF) in the posterior cingulate gyri and precunei has been reported to decrease even at a very early stage. It may be helpful to use statistical image analysis to distinguish slight decreases in rCBF in this area. We compared a 3-dimensional stereotactic surface projection (3D-SSP) technique with visual inspection in the discrimination of patients with very early AD from age-matched controls using brain perfusion SPECT. **Methods:** SPECT was obtained in 38 patients with probable AD at a very early stage and after a mean interval of 15 mo and in 76 age-matched healthy volunteers. We randomly divided these subjects into 2 groups. The first group was used to identify the areas with significant decreases of rCBF in patients compared with healthy control subjects based on the voxel-based analysis using 3D-SSP. The second group was used to compare the discrimination ability between patients and control subjects by 3D-SSP with that by visual inspection. In the second group, a *Z*-score map for a SPECT image of a subject was obtained by comparison with mean and SD SPECT images of control subjects for each voxel after anatomic standardization and voxel normalization to reference regions. Receiver operating characteristic (ROC) curves for a *Z*-score discriminating patients with AD from control subjects were analyzed in areas with significant decreases of rCBF identified in the first group. For visual inspection, 6 physicians graded the rCBF decrease on SPECT images for ROC curves. They inspected the images twice at an interval of >2 wk, and intra- and interobserver reliabilities were determined. **Results:** Visual inspection showed fair-to-excellent intra- and interobserver reliabilities. The 3D-SSP demonstrated an accuracy of 86.2% for discriminating patients with AD from control subjects when analyzing the posterior cingulate gyri and precunei with global mean normalization. In contrast, visual inspection did not show an accuracy of >74.0% for this discrimination. **Conclusion:** The ability of 3D-SSP to discriminate patients with very early AD from control subjects is superior to that of visual inspection. It is clinically useful and reliable to adopt the use of 3D-SSP as an adjunct to visual interpretation.

Key Words: Alzheimer's disease; SPECT; regional cerebral blood flow; 3-dimensional stereotactic surface projection

J Nucl Med 2004; 45:1450–1457

In a very early stage of Alzheimer's disease (AD), even before a clinical diagnosis of probable AD is possible, decreases in regional cerebral blood flow (rCBF) and glucose metabolism in the posterior cingulate gyri and precunei have been reported using PET (*1,2*) or SPECT (*3,4*). Pathologic degeneration of neurons in this area had already been reported in subjects with early AD before these neuroimaging findings became apparent (*5*). However, it is virtually impossible to distinguish a slight decrease of flow or metabolic activity in this area in subjects with early AD by visual inspection, since metabolic activity in the posterior cingulate cortex is as high as in the primary visual cortex in healthy individuals at rest (*2*). The fact that recent medications such as cholinesterase inhibitors delay the progression of AD (*6*) has increased the importance of diagnosis of AD at an earlier stage. Although recent advances in computer-assisted analysis of PET or SPECT images using 3-dimensional stereotactic surface projection (3D-SSP) (*1,2,7*) or statistical parametric mapping (SPM) (*4,8,9*) have made it

Received Aug. 9, 2003; revision accepted Jan. 28, 2004.

For correspondence or reprints contact: Hiroshi Matsuda, MD, Department of Radiology, National Center Hospital for Mental, Nervous, and Muscular Disorders, National Center of Neurology and Psychiatry 4-1-1, Ogawahigashi, Kodaira, Tokyo, 187-8551, Japan.

E-mail: matsudah@saitama-med.ac.jp

easier to detect these regional metabolic or perfusion changes, there have been few studies on the ability to discriminate early AD subjects from healthy volunteers using these stereotactic methods in the clinical setting. The purpose of our study was to compare a 3D-SSP analysis technique with visual inspection in the ability to discriminate very early AD subjects from healthy volunteers using brain perfusion SPECT.

MATERIALS AND METHODS

Subjects

We retrospectively chose 38 patients (16 men, 22 women) with a clinical diagnosis of probable AD according to the National Institute of Neurologic and Communicative Disorders and Stroke and the Alzheimer's Disease and Related Disorders Association criteria (NINCDS–ADRDA) (*10*). The patients ranged in age from 48 to 81 y, with a mean age ± SD of 71.1 ± 8.4 y. At the initial visit, they underwent thorough neuropsychologic testing (*11*) and showed selective impairment of delayed recall with no apparent loss in general cognitive, behavioral, or functional status (Table 1). They corresponded to the criteria of mild cognitive impairment (MCI) proposed by Petersen et al. (*12*) or 0.5 in Clinical Dementia Rating (*13*). Each patient underwent baseline brain perfusion SPECT at the time of the initial visit and was clinically followed-up with a second SPECT study at intervals ranging from 11.2 to 25.4 mo (mean, 15.0 mo). At the time of the baseline SPECT study, the Mini-Mental State Examination (MMSE) score (*14*) was 26.1 ± 1.6 (mean ± SD). The score significantly ($P < 0.05$; repeated measurement ANOVA with Dunnet test) decreased to 22.0 ± 3.7 at the time of the follow-up SPECT study. At the third neuropsychologic assessment without a SPECT study, except for forward and backward recall of digit span, all of the other assessments described in Table 1 were significantly ($P < 0.05$) decreased from the baseline study.

Seventy-six healthy volunteers (37 men, 39 women; age range, 67–87 y; mean age, 71.0 ± 7.1) were also studied. They had no neurologic or psychiatric disorders, including alcoholism, substance abuse, atypical headache, head trauma with loss of consciousness, or asymptomatic cerebral infarction detected by T2-weighted MRI. They did not significantly differ in age, sex, or education from the AD patients (Table 1). Spouses of the patients comprised the control subjects. They were not only spouses of the present patients but also spouses of other patients with advanced AD. These control subjects were known not to have manifested cognitive changes during the follow-up period of >2 y, since these spouses were attendant for the AD patients. We were also cognizant of their mental health. The Ethics Committee of the National Center of Neurology and Psychiatry approved this study, and all subjects gave informed consent to participate.

We randomly divided these subjects into 2 groups. The first group was used to identify the brain area with significant decreases of rCBF in patients compared with that of healthy control subjects. The second group was used then to compare the discrimination ability between patients and control subjects by 3D-SSP with that of visual inspection in regions identified in the first group.

SPECT image data in the present study have previously been reported in 12 of the 38 patients and 25 of the 76 healthy volunteers (*4*).

TABLE 1
Mean Performance Levels in Neuropsychologic Assessment

Subject	Sex F:M	Age (y)	Education (y)	Years after baseline study	MMSE	Digit span		Word learning (10 words), delayed recall (30 min)	Story recall (15 elements)		Ray–Osterrieth complex figure test		
						Forward	Backward		Immediate	Delayed (30 min)	Copy	Recall	
												Immediate	Delayed (30 min)
Healthy volunteers	39:37	71.0 ± 7.1	12.0 ± 2.7		27.8 ± 2.4	5.3 ± 0.6	4.2 ± 0.7	8.0 ± 1.0	9.6 ± 3.6	8.0 ± 2.7	35.6 ± 0.8	19.9 ± 4.3	18.8 ± 5.6
Early AD patients	22:16	71.1 ± 8.4	11.9 ± 2.6										
Baseline					26.1 ± 1.6*	5.3 ± 0.9	3.9 ± 0.8*	1.3 ± 2.2†	5.0 ± 2.6†	0.8 ± 1.7†	33.5 ± 5.7*	7.9 ± 4.4†	5.6 ± 4.9†
1st follow-up				1.2 ± 0.3	22.0 ± 3.7†‡	5.2 ± 0.9	3.8 ± 0.9†	1.2 ± 2.4†	4.5 ± 2.1†	0.5 ± 1.4†	31.2 ± 8.0†	6.8 ± 4.8†	4.1 ± 4.9†§
2nd follow-up				2.3 ± 0.6	19.9 ± 5.3†‡	5.3 ± 1.1	3.5 ± 1.2†	0.3 ± 1.1†‡	3.5 ± 2.4†‡	0.2 ± 1.1†§	29.2 ± 10.1†§	15.3 ± 5.2†‡	2.8 ± 4.2†‡

*Scores of AD patients differ from those of healthy volunteers, $P < 0.05$ (Student t test).
†Scores of AD patients differ from those of healthy volunteers, $P < 0.01$ (Student t test).
‡Scores of 1st or 2nd follow-up study differ from baseline study, $P < 0.01$ (repeated measurement ANOVA with Dunnet test as posthoc multiple comparison).
§Scores of 1st or 2nd follow-up study differ from baseline study, $P < 0.05$ (repeated measurement ANOVA with Dunnet test as posthoc multiple comparison).
Data are mean ± SD in healthy volunteers ($n = 76$) or early AD patients ($n = 38$).

SPECT

Before the SPECT scan was performed, all subjects had an intravenous line established. They were injected while lying down in the supine position with eyes closed in a dimly lit, quiet room. Each subject received an intravenous injection of 600 MBq ^{99m}Tc-ethylcysteinate dimer (^{99m}Tc-ECD). Ten minutes after the injection of ^{99m}Tc-ECD, brain SPECT was performed using triple-head rotating γ-cameras (Multispect3; Siemens Medical Systems, Inc.) equipped with high-resolution fanbeam collimators. For each camera, projection data were obtained in a 128 × 128 format for 24 angles at 50 s per angle. A Shepp and Logan Hanning filter was used for SPECT image reconstruction at 0.7 cycle/cm. Attenuation correction was performed using Chang's method.

Determination of Regions with Significant Decline of rCBF in AD

We randomly selected 19 patients and 38 healthy volunteers as the first group to establish regions with significant decline of rCBF in patients using group analysis by 3D-SSP. Each SPECT image was anatomically standardized to match a standard atlas brain (*15*) while preserving regional perfusion quantity. Maximum cortical activity was extracted to adjacent predefined surface pixels on a pixel-by-pixel basis using a 3D-SSP technique (*16*). The extracted cortical perfusion for patients was compared with that of healthy volunteers using a 2-sample Student *t* test on a pixel-by-pixel basis for approximately 16,000 predefined surface pixels covering the entire cortex. Calculated *t* values were converted to *Z* values using a probability integral transformation for comparison. A statistical significance threshold for $P = 0.05$ was calculated on the 3D-SSP *Z* map using a unified formula that controls multiple pixel comparison and a shape of the stochastic process on the 3D-SSP format (*17*).

Automated Analysis Using 3D-SSP

In the second half group, each SPECT image of the patients on both the baseline and the follow-up studies was compared with the mean and SD of SPECT images of the 38 healthy volunteers using voxel-by-voxel *Z*-score analysis after pixel normalization to values of 5 reference regions: global mean, pontine, cerebellar, sensorimotor, and thalamus; *Z* score = ([control mean] − [individual value])/(control SD) as previously reported by Minoshima et al. (*16*).

Each SPECT image of 1 of the 38 healthy volunteers was also compared with the averaged SPECT image of the remaining 37 healthy volunteers in the same manner as in the patients. Using the averaged value of positive *Z* scores in regions with significant decline of rCBF identified in the first group as the threshold, receiver operating characteristic (ROC) curves were determined using the ROCKIT 0.9β program developed by Metz et al. (http://xray.bsd.uchicago.edu/krl) (*18*). The program calculates the area under the ROC curves (Az), accuracy, sensitivity, and specificity. Accuracy was determined as the value at the point where the sensitivity is the same as the specificity on the ROC curve. The program also tests differences in Az between 3D-SSP and visual inspection. The Games–Howell test was used as the multiple comparison method of Az for specific areas and reference regions. Then, using the PlotROC program (http://xray.bsd.uchicago.edu/krl), interpolated values were also statistically calculated for drawing ROC curves.

Analysis with Visual Inspection

The observers comprised 6 medical doctors with experience in nuclear medicine for at least a year: 4 diagnostic radiologists with careers extending to 20, 16, 6, and 3 y, and 2 physicians working in nuclear medicine for 4 y and 1 y. Before the observers worked independently, a 10-min explanation was provided with regions identified in the first group, which were shown to teach where rCBF typically decreases in AD patients in the early stage. After this teaching session, transaxial, coronal, and sagittal sections of the original SPECT images in the second group were randomly presented to the observers. All of the observers were informed that these SPECT images originated from early AD patients and healthy volunteers. Images of healthy volunteers were intermingled with images of patients. The observers scaled the rCBF decrease into 5 levels in all of the specific areas. Five categories (definite decrease, possible decrease, equivocal decrease, possibly no decrease, and definitely no decrease) were used to describe these 5 levels of brain perfusion decrease. Finally, the observers also judged whether the presented SPECT images were those of the AD patients with 5 categories of certainty: definitely, possibly, equivocally, possibly no, and definitely no. To take the intraobserver variance into account, the observers judged the images twice in the same manner at intervals of >2 wk.

For the intra- and interobserver reliability trials, Spearman ρ-scores and 2-way random-effect intraclass correlation coefficients (ICCs) were calculated using SPSS statistical software (SPSS Inc.). These scores and coefficients for all images of AD patients and healthy volunteers were calculated separately in each specific area. ICC values of <0.4 were deemed as representing poor reliability, 0.4–0.75 as fair to good reliability, and >0.75 as excellent reliability.

RESULTS

Determination of Regions with Significant Decline of rCBF in AD

In the first group, the group comparison at the baseline study showed a significant ($P < 0.05$) rCBF reduction in 2 specific areas—namely, the posterior cingulate gyri and precunei and parietal association cortex. The follow-up SPECT study revealed 3 additional specific areas with rCBF reduction: lower and medial temporal areas, temporal association cortex, and anterior cingulate gyri (Fig. 1). Regions of interest (ROIs) were drawn over 5 specific areas (Fig. 2) using OSIRIS (University Hospital of Geneva, Geneva, Switzerland) with the consent of 2 operators: (1) 2 ROIs in bilateral medial views for the posterior cingulate gyri and precunei; (2) 6 ROIs in bilateral lateral, medial, and inferior views for lower and medial temporal areas; (3) 6 ROIs in bilateral lateral, superior, and posterior views for parietal association cortex; (4) 4 ROIs in bilateral lateral and posterior views for temporal association cortex; and (5) 2 ROIs in bilateral medial views for anterior cingulate gyri. ROI sizes ranged from 54 to 543 pixels. These ROIs were confirmed to be at a quite similar location wherever the reference area for pixel normalization was chosen.

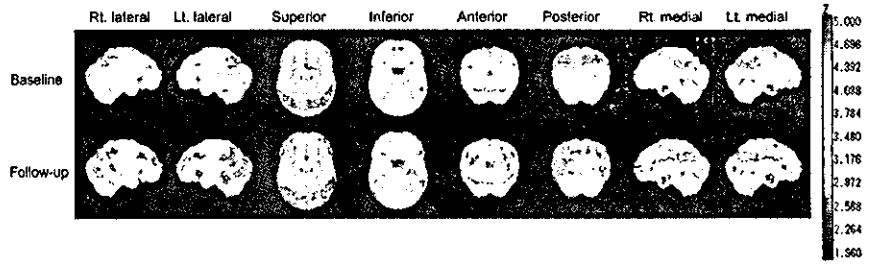

FIGURE 1. Decrease of rCBF adjusted to global mean cerebral blood flow, shown by group analysis of 3D-SSP in patients with early AD at baseline study (top row) and follow-up study (bottom row) compared with healthy volunteers ($P < 0.05$, with multiple comparisons). Rt. = right; Lt. = left.

Comparative Analysis of ROC Curves Between 3D-SSP and Visual Inspection

Table 2 shows Az by 3D-SSP with SEs for 5 specific areas with different reference regions. We averaged positive Z-score values across the pixels within each ROI and then chose the highest value among these averaged Z scores in ROIs belonging to each specific area. There were no significant differences in Az among the reference regions used for pixel normalization after pooling specific areas at both the baseline and follow-up studies. At the baseline study, although there were no significant differences in Az among the specific areas after pooling reference regions, posterior cingulate gyri and precunei showed greater Az than any other specific area with any reference region. At the follow-up study, posterior cingulate gyri and precunei still showed greater Az than other specific areas except for lower and medial temporal areas. From these results, Az for discrimination of AD patients and control subjects by 3D-SSP was defined as the same value as Az for posterior cingulate gyri and precunei with global mean normalization.

In visual inspection, significant ρ-scores between the first and second trials ($P < 0.01$) indicate good intraobserver reliabilities (Fig. 3). Excellent interobserver reliabilities ranging from 0.762 to 0.890 were observed in every specific area and in discrimination of AD patients and control subjects (Table 3).

The ROC curves for discrimination of AD patients and control subjects were compared between 3D-SSP and visual inspection (Fig. 4). Az values for 3D-SSP in the posterior cingulate gyri were greater than those for visual inspection.

In Figure 5, Az values of the first trial of visual inspection were compared with Az values of 3D-SSP with global mean normalization. At the baseline study, 3D-SSP results in the posterior cingulate gyri and precunei showed significantly higher Az ($P < 0.05$) than results by visual inspection for the discrimination of AD patients and control subjects in all observers. At the follow-up study, all observers showed lower Az values for the discrimination than 3D-SSP. In all specific areas, Az values of all observers were lower than those of 3D-SSP at both the baseline and the follow-up studies.

Table 4 shows the accuracy when sensitivity is equal to specificity. In 3D-SSP, the maximum accuracy of 86.2% was obtained in the posterior cingulate gyri and precunei with reference to the global mean. This accuracy was higher than the maximum accuracy of 74.0% in visual inspection for the discrimination of AD patients and control subjects at the baseline study. At the follow-up study, an accuracy of 74.0% was observed in the posterior cingulate gyri and precunei with reference to the global mean in 3D-SSP, which is still higher than the maximum accuracy of 65.9% in visual inspection.

DISCUSSION

Burdette et al. (*7*) corroborated improvement of diagnostic performance using 3D-SSP in an ^{18}FDG PET study on probable AD patients. In the present study, we confirmed this improvement in AD patients limited to the very early stage using ^{99m}Tc-ECD SPECT, which is more widely performed than PET worldwide. 3D-SSP has been reported to be less affected by the presence of atrophy than SPM (*19*). This method yielded a higher accuracy, even in parietal association cortical areas, than visual inspection, in which metabolic reduction is reported to be the best discriminator of patients with probable AD from healthy volunteers (*16*).

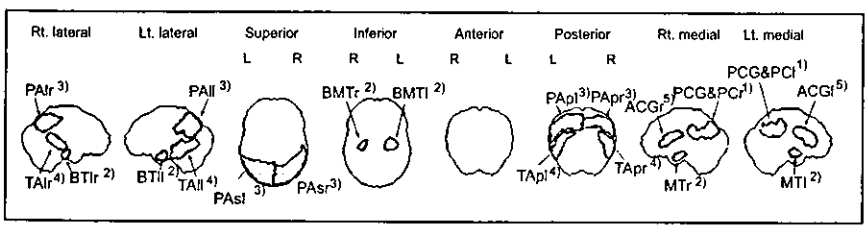

FIGURE 2. ROIs drawn over areas with significant decrease of rCBF in early AD. ROIs were classified into 5 specific areas as follows (numbers with open parentheses denote numbers of pixels included in ROIs): (1) posterior cingulate gyri and precunei: PCG&PC (r = 321 pixels, l = 280 pixels); (2) lower and medial temporal areas: MT (medial temporal areas) (r = 82 pixels, l = 79 pixels), BMT (basal medial temporal area) (r = 60 pixels, l = 112 pixels), and BTl (lateral basal temporal area) (r = 54 pixels, l = 74 pixels); (3) parietal association cortex: PAl (lateral parietal association cortex) (r = 279 pixels, l = 174 pixels), PAp (posterior parietal association cortex) (r = 320 pixels, l = 439 pixels), and Pas (superior parietal association cortex) (r = 543 pixels, l = 496 pixels); (4) temporal association cortex: TAl (lateral temporal association cortex) (r = 172 pixels, l = 367 pixels), TAp (posterior temporal association cortex) (r = 223 pixels, l = 241 pixels); (5) anterior cingulate gyri: ACG (r = 188 pixels, l = 256 pixels).

TABLE 2
Areas Under ROC Curves (Az) for Specific Areas with Different Reference Regions Obtained from 3D-SSP Analysis

Baseline study reference region	Az of specific area				
	PCG&PC	PA	MT	TA	ACG
Global mean	0.937 (0.035)	0.786 (0.080)	0.801 (0.064)	0.766 (0.074)	0.782 (0.065)
Pons	0.814 (0.067)	0.717 (0.076)	0.670 (0.078)	0.605 (0.084)	0.756 (0.066)
Cerebellum	0.897 (0.046)	0.825 (0.063)	0.830 (0.058)	0.768 (0.066)	0.791 (0.066)
Sensorimotor	0.794 (0.059)	0.661 (0.072)	0.605 (0.086)	0.462 (0.087)	0.704 (0.072)
Thalamus	0.819 (0.060)	0.743 (0.070)	0.690 (0.080)	0.662 (0.071)	0.698 (0.082)
Follow-up study reference region	**Az of specific area**				
	PC	PA	MT	TA	ACG
Global mean	0.839 (0.060)	0.807 (0.063)	0.844 (0.057)	0.801 (0.066)	0.781 (0.069)
Pons	0.833 (0.058)	0.760 (0.068)	0.817 (0.063)	0.753 (0.073)	0.823 (0.060)
Cerebellum	0.836 (0.061)	0.797 (0.067)	0.848 (0.051)	0.833 (0.060)	0.817 (0.063)
Sensorimotor	0.846 (0.056)	0.700 (0.069)	0.794 (0.065)	0.717 (0.080)	0.809 (0.061)
Thalamus	0.868 (0.049)	0.748 (0.067)	0.816 (0.058)	0.758 (0.069)	0.799 (0.064)

PCG&PC = posterior cingulate gyri and precunei; PA = parietal association cortex; MT = lower and medial temporal areas; TA = temporal association cortex; ACG = anterior cingulate gyri.

Data are areas under ROC curves (Az) obtained from 3D-SSP. Numbers in parentheses are of Az. No significant results were observed among reference regions after pooling specific areas using Games–Howell test.

The flow or metabolic reduction in the posterior cingulate gyri and precunei has been established to characterize early-to-moderate AD even after correction of partial-volume effects using segmented MR images (*20*). The present study using 3D-SSP demonstrated that rCBF reduction in this specific area is the most reliable finding for diagnosing very early AD, with a high accuracy of 86.2%. 3D-SSP showed a significantly higher performance than the experienced observers at the baseline study. This specific area is known to be important in memory (*21*). A PET study revealed activation of the retrosplenial area of the cingulate cortex during the episodic memory-encoding tasks (*22*). Clinical evidence of the existence of a brain tumor (*23*) or arteriovenous malformation (*24*) in the retrosplenial cingulate cortex supports the importance of this area in memory function.

Most previous pathologic and morphologic studies suggested that structures within the medial temporal structures—amygdala, hippocampal formation, entorhinal cortex, and parahippocampal and fusiform gyri—are the first to be affected in AD with histologic changes, including amy-

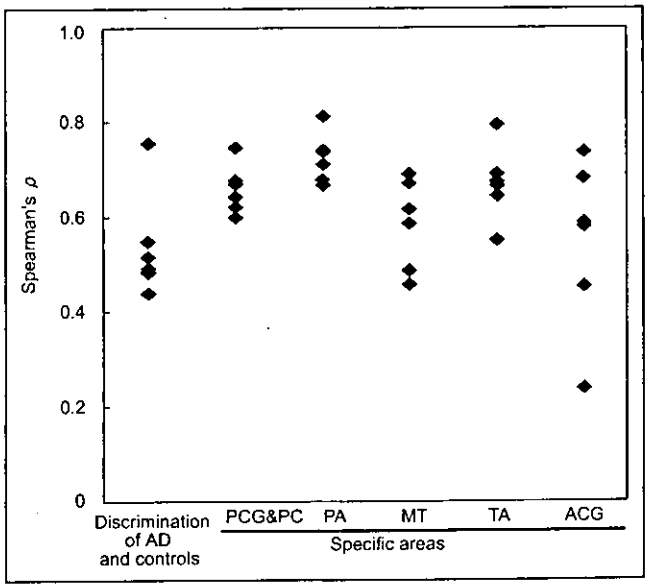

FIGURE 3. Intraobserver reliability between 1st and 2nd trials. ◆, Spearman ρ for individual observer. PCG&PC = posterior cingulate gyri and precunei; PA = parietal association cortex; MT = lower and medial temporal areas; TA = temporal association cortex; ACG = anterior cingulate gyri.

TABLE 3
Interobserver Reliability of Observers

Parameter	Interobserver reliability	
	ICC	95% CI
Discrimination of AD patients and control subjects	0.826	(0.777, 0.867)
Specific area		
PCG&PC	0.805	(0.748, 0.852)
PA	0.890	(0.857, 0.917)
MT	0.819	(0.760, 0.866)
TA	0.864	(0.810, 0.903)
ACG	0.762	(0.649, 0.836)

PCG&PC = posterior cingulate gyri and precunei; PA = parietal association cortex; MT = lower and medial temporal areas; TA = temporal association cortex; ACG = anterior cingulate gyri.

Data in parentheses are 95% confidence intervals (CIs).

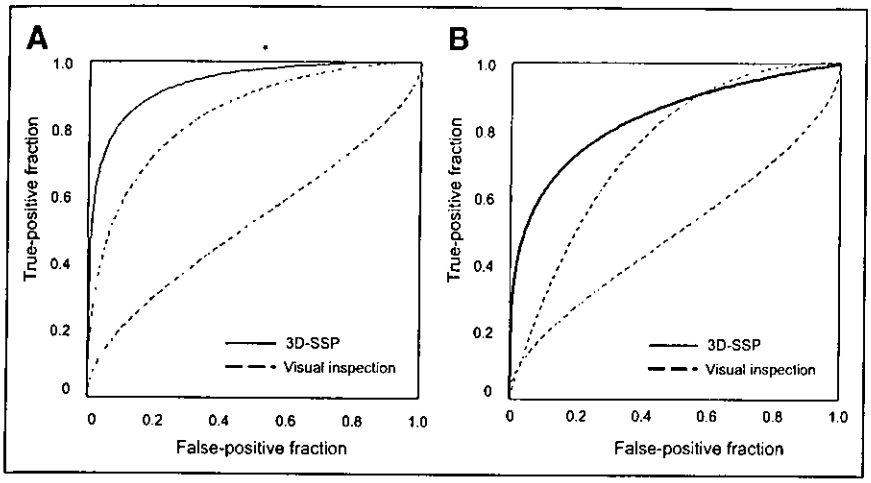

FIGURE 4. ROC curves obtained from 3D-SSP with global mean normalization when thresholding at highest value among averaged positive *Z* scores for ROIs belonging to posterior cingulate gyri and precunei and ROC curves for discrimination of AD patients and control subjects obtained from most excellent and poorest observers for either first or second reading. (A) Baseline study. (B) Follow-up study.

loid deposits and neurofibrillary changes (*5,25–27*). The reduced rCBF in the medial temporal structures demonstrated by PET (*27*) or by a recent high-resolution SPECT system is consistent with these pathologic findings (*28,29*). In the present study, 3D-SSP revealed rCBF reduction in the lower and medial temporal areas more accurately in the follow-up study than in the baseline study. This finding is consistent with our longitudinal results using SPM, in which a significant reduction of hippocampal blood flow did not appear until the mean score of MMSE decreased from 26.2 to 22.3 (*4*). Even in the follow-up study, visual inspection showed significantly lower performance in this specific area than 3D-SSP. This may be because of inherent low accumulation of ^{99m}Tc-ECD in the medial temporal lobes (*30*).

In the present study, rCBF decrease was observed in the anterior cingulate gyri, as well as the posterior cingulate gyri, more prominently in the follow-up study. After involvement of the medial temporal structures, neuropathologic findings such as amyloid deposits and neurofibrillary changes have been observed to spread to the basal forebrain and anterior cingulate gyri, even in the clinically incipient stage of AD, becoming more conspicuous as the disease progresses (*31*). Decreased rCBF in the anterior cingulate gyrus has been reported in subjects with questionable AD at baseline SPECT who converted to AD on follow-up (*3*). Attention must be paid to the possibility of pseudo rCBF reduction produced in structures near the dilated ventricles by mismatches at the edges of the ventricles (*19*). However, for the clinical purpose of diagnosing AD, partial-volume effects may increase the sensitivity of detection of rCBF reduction. Current evidence suggests that after an initial amnesic stage in AD, attention is the first nonmemory domain to be affected before deficits in language and visuospatial function (*32*). In AD it appears that divided attention is particularly vulnerable, while sustained attention is relatively well preserved in the early stages (*32,33*). It has been reported that divided attention activates the anterior cingulate gyri, though sustained attention does not (*34,35*).

Concerning the reference regions for pixel normalization in 3D-SSP, Minoshima et al. reported that the pons is a

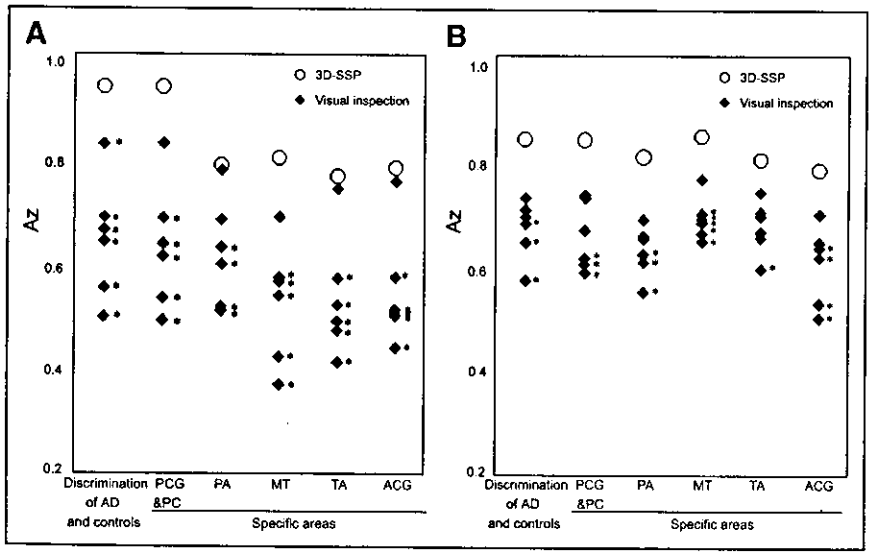

FIGURE 5. Comparison of Az between observers' first visual inspection and 3D-SSP with global mean normalization. ◆, Az for individual observer; ○, Az for 3D-SSP. (A) Baseline study. (B) Follow-up study. PCG&PC = posterior cingulate gyri and precunei; PA = parietal association cortex; MT = lower and medial temporal areas; TA = temporal association cortex; ACG = anterior cingulate gyri. *Az of visual inspection is lower than Az by 3D-SSP analysis ($P < 0.05$). Statistical significance between Az values was calculated using ROCKIT program (*18*).

TABLE 4
Accuracies of Observers' Visual Inspection and 3D-SSP Analysis

Baseline study	Accuracies of discrimination of AD patients and control subjects	Accuracies of specific areas				
		PCG&PC	PA	MT	TA	ACG
Visual inspection	0.493–0.740	0.495–0.735	0.487–0.687	0.387–0.618	0.417–0.660	0.437–0.672
3D-SSP reference region						
Global mean	0.862	0.862	0.718	0.712	0.679	0.689
Pons		0.722	0.639	0.602	0.556	0.668
Cerebellum		0.795	0.729	0.730	0.678	0.698
Sensorimotor		0.702	0.599	0.556	0.453	0.573
Thalamus		0.720	0.658	0.618	0.600	0.628
Follow-up study	**Accuracies of discrimination of AD patients and control subjects**	**Accuracies of specific areas**				
		PCG&PC	PA	MT	TA	ACG
Visual inspection	0.530–0.659	0.541–0.654	0.538–0.616	0.585–0.676	0.547–0.661	0.479–0.622
3D-SSP reference region						
Global mean	0.740	0.740	0.710	0.744	0.706	0.690
Pons		0.733	0.671	0.72	0.667	0.742
Cerebellum		0.738	0.703	0.766	0.734	0.720
Sensorimotor		0.745	0.631	0.7	0.641	0.711
Thalamus		0.765	0.662	0.719	0.669	0.704

PCG&PC = posterior cingulate gyri and precunei; PA = parietal association cortex; MT = lower and medial temporal areas; TA = temporal association cortex; ACG = anterior cingulate gyri.

Data are accuracies when sensitivity is equal to specificity in ROC analysis. Accuracies of visual inspection are described as a range from minimum to maximum at the first trial.

reliable reference for data normalization on quantitative ^{18}F-FDG PET measurement (*36*). In our study, Az did not show significant differences among reference regions. In the case of SPECT, the pons may be at the margin of spatial resolution for adequate and stable counts. Although rCBF in the cerebellum has been reported to decrease in advanced AD patients (*37*), the choice of cerebellum for pixel normalization would be acceptable in mild or very early AD. Subsequently, Minoshima et al. used the thalamus as a reference region (*16*) based on their prior observation that the thalamus or primary sensorimotor cortex is more suitable than the global mean or cerebellum. They also reported that the thalamus has a distinct shape and is located just above the intercommissural line, the standard line defining the stereotactic coordinate system, thereby ensuring reliable and accurate localization. Bartenstein et al. (*38*) used thalamic normalization even though they showed that global normalization resulted in the least mean cortical coefficients of variation in ^{99m}Tc-ECD SPECT. They considered global normalization to be inappropriate for a disease such as AD with widespread metabolic or flow reduction and concluded that the thalamus is the most robust reference region for SPECT images. However, the thalamus is pathologically known to be involved from an early stage (*25*). Moreover, Johnson et al. (*3*) revealed a rCBF decrease in the anterior thalamus in subjects with questionable AD at baseline SPECT who converted to AD on follow-up. We considered that global normalization is sufficient for routine clinical discrimination of early AD patients and control subjects. The present results confirmed the highest accuracy using global normalization at the baseline study.

Finally, we must refer to limitations of this kind of study even when conducted in the best situation (a specialized clinic for memory disorders). It has been reported that the clinical diagnosis of probable AD is 80%–90% accurate when compared with final pathologic verification (*39*), although prolonged follow-up with serial evaluation was performed to diagnose AD clinically in the present study.

CONCLUSION

A 3D-SSP technique using a normal database of brain perfusion SPECT images can detect a slight rCBF decrease in the posterior cingulate gyri and precunei with higher ability to discriminate very early AD patients from healthy control subjects than visual inspection. This technique afforded the maximum discrimination of 86.2% in accuracy at the very early stage corresponding to MCI. On the other hand, the maximum accuracy of visual interpretation was >10% lower as compared with 3D-SSP. The present results suggest that it is clinically useful and reliable to adopt the use of artificial computer intelligence as an adjunct to visual image interpretation for dementia evaluation.

ACKNOWLEDGMENTS

This study was supported by Comprehensive Research on Aging and Health, grant H13-choju-004 from the Ministry of Health, Labor and Welfare. The authors are very thankful to Prof. Satoshi Minoshima (University of Washington) and Dr. Toru Matsumoto (National Institute of Radiologic Sciences) for valuable suggestions regarding the theory of 3D-SSP and ROC curve analysis, respectively; Dr. Toru Kinoshita (Department of Biostatistics, School of Health Sciences and Nursing, University of Tokyo) for statistics; John Gelblum for proofreading this manuscript; and the technical staff in our hospital for data acquisition.

REFERENCES

1. Minoshima S, Foster NL, Kuhl DE. Posterior cingulate cortex in Alzheimer's disease. *Lancet.* 1994;344:895.
2. Minoshima S, Giordani B, Berent S, et al. Metabolic reduction in the posterior cingulate cortex in very early Alzheimer's disease. *Ann Neurol.* 1997;42:85–94.
3. Johnson KA, Jones BL, Holman JA, et al. Preclinical prediction of Alzheimer's disease using SPECT. *Neurology.* 1998;50:1563–1571.
4. Kogure D, Matsuda H, Ohnishi T, et al. Longitudinal evaluation of early Alzheimer's disease using brain perfusion SPECT. *J Nucl Med.* 2000;41:1155–1162.
5. Brun A, Gustafson L. Distribution of cerebral degeneration in Alzheimer's disease: a clinico-pathological study. *Arch Psychiatr Nervenkr.* 1976;223:15–33.
6. Gerard E, Konrad B, Colin LM, Jean-Marie M. Prospects for pharmacological intervention in Alzheimer disease. *Arch Neurol.* 2000;57:454–459.
7. Burdette JH, Minoshima S, Borght TV, Tran DD, Kuhl DE. Alzheimer disease: improved visual interpretation of PET images by three-dimensional stereotaxic surface projections. *Radiology.* 1996;198:837–843.
8. Frackowiak RSJ, Friston KJ, Frith CD, Dolan RJ, Mazziotta JC. *Human Brain Function.* 1st ed. San Diego, CA: Academic Press; 1997.
9. Ishii K, Sasaki M, Yamaji S, Sakamoto S, Kitagaki H, Mori E. Demonstration of decreased posterior cingulate gyrus correlates with disorientation for time and place in Alzheimer's disease by means of $H_2{}^{15}O$ positron emission tomography. *Eur J Nucl Med.* 1997;24:670–673.
10. McKhann G, Drachman D, Folstein M, Katzman R, Prie D, Stadlan EM. Clinical diagnosis of Alzheimer's disease: report of the NINCDS-ADRDA Work Group under the auspices of Department of Health and Human Services Task Force on Alzheimer's Disease. *Neurology.* 1984;34:939–944.
11. Hodges JR. *Cognitive Assessment for Clinicians.* 1st ed. Oxford, U.K.: Oxford Medical Publication; 1993.
12. Petersen RC, Dooby R, Kurz A, et al. Current concepts in mild cognitive impairment. *Arch Neurol.* 2001;58:1985–1992.
13. Hughes CP, Berg L, Danziger WL, Coben LA, Martin RL. A new clinical scale for the staging of dementia. *Br J Psychiatry.* 1982;140:566–572.
14. Folstein MF, Folstein SE, McHugh PR. Mini-Mental State: a practical method for grading the cognitive state of patients for the clinician. *J Psychiatr Res.* 1975; 12:189–198.
15. Minoshima S, Koeppe RA, Frey KA, Kuhl DE. Anatomic standardization: linear scaling and nonlinear warping of functional brain images. *J Nucl Med.* 1994;3: 1528–1537.
16. Minoshima S, Frey KA, Koeppe RA, et al. A diagnostic approach in Alzheimer's disease using three-dimensional stereotactic surface projections of fluorine-18-FDG PET. *J Nucl Med.* 1995;36:1238–1248.
17. Worsley KJ, Marrett S, Neelin P, et al. A unified statistical approach for determining significant signals in location and scale space images of cerebral activation. In: Myers R, Cunningham V, Baily D, et al, eds. *Quantification of Brain Function Using PET.* San Diego, CA: Academic Press; 1996:327–333.
18. Metz CE, Herman BA, Roe CA. Statistical comparison of two ROC-curve estimates obtained from partially-paired datasets. *Med Decis Making.* 1998;18: 110–121.
19. Ishii K, Willoch F, Minoshima S, et al. Statistical brain mapping of ^{18}F-FDG PET in Alzheimer's disease: validation of anatomic standardization for atrophied brains. *J Nucl Med.* 2001;42:548–557.
20. Ibanez V, Pietrini P, Alexandar GE, et al. Regional glucose metabolic abnormalities are not the result of atrophy in Alzheimer's disease. *Neurology.* 1998;50: 1585–1593.
21. Desgranges B, Baron JC, de la Sayette V, et al. The neural substrates of memory systems impairment in Alzheimer's disease: a PET study of resting brain glucose utilization. *Brain.* 1998;121:611–631.
22. Fletcher PC, Frith CD, Grasby PM, Shallice T, Frackwiak RSJ, Dolan RJ. Brain system for encoding and retrieval of auditory-verbal memory. *Brain.* 1995;118: 401–416.
23. Rudge P, Warrington EK. Selective impairment of memory and visual perception in splenial tumours. *Brain.* 1991;114:349–360.
24. Valenstein E, Bowers D, Verfaellie M, Heilman KM, Day A, Watson RT. Retrosplenial amnesia. *Brain.* 1987;110:1631–1646.
25. Braak H, Braak E. Neuropathological staging of Alzheimer-related changes. *Acta Neuropathologica.* 1991;82:239–256.
26. Gomez-Isla T, Price TL, McKeel DW, Morris JC, Growdon JH, Hyman BT. Profound loss of layer II entorhinal cortex neurons occurs in very mild Alzheimer's disease. *J Neurosci.* 1996;16:4491–4500.
27. Pearlson GD, Harris GJ, Powers RE, et al. Quantitative changes in mesial temporal volume, regional cerebral blood flow, and cognition in Alzheimer's disease. *Arch Gen Psychiatry.* 1992;49:402–408.
28. Ohnishi T, Hoshi H, Nagamachi S, et al. High-resolution SPECT to assess hippocampal perfusion in neuropsychiatric diseases. *J Nucl Med.* 1995;36:1163–1169.
29. Julin P, Lindqvist J, Svensson L, Slomka P, Wahlund LO. MRI-guided SPECT measurements of medial temporal lobe blood flow in Alzheimer's disease. *J Nucl Med.* 1997;38:914–919.
30. Oku N, Matsumoto M, Hashikawa K, et al. Intra-individual differences between technetium-99m-HMPAO and technetium-99m-ECD in the normal medial temporal lobe. *J Nucl Med.* 1997;38:1109–1111.
31. Jack CR, Petersen RC, Xu YC, et al. Medial temporal atrophy on MRI in normal aging and very mild Alzheimer's disease. *Neurology.* 1997;49:786–794.
32. Perry RJ, Hodges JR. Attention and executive deficits in Alzheimer's disease: a critical review. *Brain.* 1999;122:383–404.
33. Rizzo M, Anderson SW, Dawson J, Myers R, Ball K. Visual attention impairments in Alzheimer's disease. *Neurology.* 2000;54:1954–1959.
34. Corbetta M, Miezin FM, Dobmeyer S, Shulman GL, Pertersen SE. Selective and divided attention during visual discrimination of shape, color, and speed: functional anatomy by positron emission tomography. *J Neurosci.* 1991;11:2383–2402.
35. Iidaka T, Anderson ND, Kapur S, Cabeza R, Craok FI. The effect of divided attention on encoding and retrieval in episodic memory revealed by positron emission tomography. *J Cogn Neurosci.* 2000;12:267–280.
36. Minoshima S, Frey KA, Foster NL, Kuhl DE. Preserved pontine glucose metabolism in Alzheimer disease: a reference region for functional brain image (PET) analysis. *J Comput Assist Tomogr.* 1995;19:541–547.
37. Ishii K, Sasaki M, Kitagaki H, et al. Reduction of cerebellar glucose metabolism in advanced Alzheimer's disease. *J Nucl Med.* 1997;38:925–928.
38. Bartenstein P, Minoshima S, Hirsch C, et al. Quantitative assessment of cerebral blood flow in patients with Alzheimer's disease by SPECT. *J Nucl Med.* 1997; 38:1095–1101.
39. Adams RD. Alzheimer's disease. In: Adams RD, Victor M, Ropper AH, eds. *Principles of Neurology.* 6th ed. New York, NY: McGraw-Hill; 1997:1049–1057.

Effects of partial volume correction on discrimination between very early Alzheimer's dementia and controls using brain perfusion SPECT

Hidekazu Kanetaka[1,4], Hiroshi Matsuda[1], Takashi Asada[2], Takashi Ohnishi[1], Fumio Yamashita[2], Etsuko Imabayashi[1], Fumiko Tanaka[1], Seigo Nakano[3], Masaru Takasaki[4]

[1] Department of Radiology, National Center Hospital for Mental, Nervous and Muscular Disorders, National Center of Neurology and Psychiatry, Kodaira, Tokyo, Japan
[2] Department of Neuropsychiatry, Institute of Clinical Medicine, University of Tsukuba, Tsukuba, Ibaraki, Japan
[3] Department of Geriatric Medicine, National Center Hospital for Mental, Nervous and Muscular Disorders, National Center of Neurology and Psychiatry, Kodaira, Tokyo, Japan
[4] Department of Geriatric Medicine, Tokyo Medical University, Shinjuku, Tokyo, Japan

Received: 25 December 2003 / Accepted: 9 February 2004 / Published online: 28 February 2004

Abstract. We assessed the accuracy of brain perfusion single-photon emission computed tomography (SPECT) in discriminating between patients with probable Alzheimer's disease (AD) at the very early stage and age-matched controls before and after partial volume correction (PVC). Three-dimensional MRI was used for PVC. We randomly divided the subjects into two groups. The first group, comprising 30 patients and 30 healthy volunteers, was used to identify the brain area with the most significant decrease in regional cerebral blood flow (rCBF) in patients compared with normal controls based on the voxel-based analysis of a group comparison. The second group, comprising 31 patients and 31 healthy volunteers, was used to study the improvement in diagnostic accuracy provided by PVC. A Z score map for a SPECT image of a subject was obtained by comparison with mean and standard deviation SPECT images of the healthy volunteers for each voxel after anatomical standardization and voxel normalization to global mean or cerebellar values using the following equation: Z score = ([control mean]–[individual value])/(control SD). Analysis of receiver operating characteristics curves for a Z score discriminating AD and controls in the posterior cingulate gyrus, where a significant decrease in rCBF was identified in the first group, showed that the PVC significantly enhanced the accuracy of the SPECT diagnosis of very early AD from 73.9% to 83.7% with global mean normalization. The PVC mildly enhanced the accuracy from 73.1% to 76.3% with cerebellar normalization. This result suggests that early diagnosis of AD requires PVC in a SPECT study.

Keywords: SPECT – Alzheimer's disease – Regional cerebral blood flow – ^{99m}Tc-ECD – Partial volume correction

Eur J Nucl Med Mol Imaging (2004) 31:975–980
DOI 10.1007/s00259-004-1491-3

Hiroshi Matsuda (✉)
Department of Radiology,
National Center Hospital for Mental,
Nervous and Muscular Disorders,
National Center of Neurology and Psychiatry,
4-1-1 Ogawahigashi, 187-8551 Kodaira, Tokyo, Japan
e-mail: matsudah@ncnpmusashi.gr.jp
Tel.: +81-42-3412711, Fax: +81-42-3461736

Introduction

The fact that recently available medications such as cholinesterase inhibitors delay the progression of Alzheimer's disease (AD) has increased the urgency of diagnosing AD at an earlier stage. Although recent advances in the computer-assisted statistical analysis of positron emission tomography (PET) or single-photon emission computed tomography (SPECT) after anatomical image standardization have made it easier to detect regional metabolic or perfusion changes in the early stage of AD [1, 2, 3, 4], there have been few studies on the diagnostic performance of SPECT in very early AD.

The more limited spatial resolution of SPECT scanners as compared with that of PET does not allow an exact measurement of the local radiotracer concentration in brain tissue since partial volume effects cause underestimation of activity in small structures of the brain. Since brain atrophy accentuates the partial volume effects on SPECT measurements, actual regional cerebral blood

flow (rCBF) could be underestimated in AD. We have already reported which brain structures show the greatest influence of partial volume effects in SPECT studies on AD patients [5, 6] and aged healthy men [7]. The present SPECT study was undertaken to evaluate whether partial volume correction (PVC) improves discrimination between AD patients and controls by automated analysis of brain perfusion SPECT.

Materials and methods

Study participants. We retrospectively chose 61 patients (32 men and 29 women) with a clinical diagnosis of probable AD according to the National Institute of Neurological and Communicative Disorders and Stroke and the Alzheimer's Disease and Related Disorders Association criteria (NINCDS-ADRDA) [8]. At the initial visit, the patients showed selective impairment of delayed recall with no apparent loss in general cognitive, behavioral, or functional status and corresponded to the criteria of mild cognitive impairment (MCI) proposed by Petersen et al. [9] or 0.5 in Clinical Dementia Rating [10]. They ranged in age from 48 to 87 years with a mean±standard deviation (SD) of 70.6±8.4. The Mini-Mental State Examination (MMSE) [11] score ranged from 24 to 29 (mean±SD 26.0±1.5) at the initial visit. During the subsequent follow-up period of 2–6 years, the subjects showed progressive cognitive decline and eventually fulfilled the diagnosis of probable AD according to the NINCDS-ADRDA criteria.

Sixty-one control subjects (30 men and 31 women; age 54–86 years, mean±SD 70.2±7.3 years) were healthy volunteers with no memory impairment or cognitive disorders. Their performance was within normal limits both on the Wechsler Memory Scale-Revised and on the Wechsler Adult Intelligence Scale-Revised. The MMSE score ranged from 26 to 30 (mean±SD 28.7±1.5). They did not differ significantly in age or education from the AD patients. The Ethics Committee of the National Center of Neurology and Psychiatry approved this study for healthy volunteers, all of whom gave their informed consent to participation.

All of subjects were right handed and screened by questionnaire and medical history to exclude those with medical conditions potentially affecting the central nervous system. In addition, none of them had asymptomatic cerebral infarction detected by T2-weighted MRI.

We randomly divided these subjects into two groups. The first group was used to identify the brain area with the most significant decrease in rCBF in patients compared with normal controls. Then, the second group was used to study the improvement in diagnostic accuracy provided by PVC only in the region identified in the first group.

SPECT study and PVC. All of the subjects underwent both brain perfusion SPECT and MRI, in patients within 2 months after the initial visit. Before SPECT was performed, an intravenous line was established in all subjects. They were injected while lying in the supine position with the eyes closed in a dimly lit, quiet room. Each received a 600 MBq intravenous injection of ^{99m}Tc-ethyl cysteinate dimer (^{99m}Tc-ECD). Ten minutes after the injection of ^{99m}Tc-ECD, brain SPECT was performed using cameras equipped with high-resolution fanbeam collimators (Multispect3; Siemens Medical Systems, Ic, Hoffman Estates, IL). A Shepp and Logan Hanning filter was used as a filtered back-projection method for SPECT image reconstruction at 0.7 cycles/cm. Attenuation correction was performed using Chang's method with an optimized effective attenuation coefficient of 0.09 cm^{-1}.

Correction for PVE was performed for atrophy correction in SPECT images using three-dimensional volumetric T1-weighted MR images (a 1.0-Tesla system, Magnetom Impact Expert, Siemens, Erlangen, Germany) as described in previous studies [5, 6, 7,12,13]. In summary, the PVC was performed by dividing a gray matter SPECT image by a gray matter MR image that was segmented from an original MR image and further convoluted with equivalent spatial resolution to SPECT on a voxel-by-voxel basis. In the present study, a fully automated program for the PVC was developed using C++ language.

Determination of a region with significant decline in rCBF in AD. We randomly selected 30 patients and 30 healthy volunteers as the first group to establish a region with a significant decline in rCBF in patients using statistical parametric mapping 99 (SPM99) (Wellcome Department of Cognitive Neurology, London, UK). Gray matter SPECT images before and after PVC were spatially normalized in SPM99 to a standardized stereotactic space based on the Talairach and Tournoux atlas [14], using 12-parameter linear affine normalization and a further 12 nonlinear iteration algorithms with an original template for ^{99m}Tc-ECD [15]. Then, images were smoothed using a 12-mm FWHM isotropic Gaussian kernel.

The patients and healthy volunteers were compared before and after PVC using the "compare-population one scan/subject" routine in SPM99. The "proportional scaling" routine was used to control for individual variation in global ^{99m}Tc-ECD uptake; these data will be referred to as "adjusted rCBF." The resulting set of values for each contrast constituted a statistical parametric map of the t statistic SPM$\{t\}$. The SPM(t) were transformed to the unit normal distribution {SPM(Z)} and thresholded at P<0.001. The significance of each region was estimated with a threshold of P=0.05 with correction for multiple non-independent comparisons. Extent threshold was set to 0 voxel.

Automated analysis using a Z score map. A software program for analysis of SPECT images was developed to discriminate between the rest of the 31 patients and 31 healthy volunteers as the second group. Each SPECT image of the patients was compared with the mean and SD of SPECT images of the 31 healthy volunteers using voxel-by-voxel Z score analysis after voxel normalization to global mean or cerebellar values; Z score = ([control mean]−[individual value])/(control SD) as previously reported by Minoshima et al. [16] and Ishii et al. [17]. We calculated the SD of the control database before and after PVC with voxel normalization to global mean and cerebellar values in already defined regions in the first group with a significant decline in rCBF in patients. These Z score maps were displayed by overlay on tomographic sections and by projection with an averaged Z score of 14 mm thickness to surface rendering of the anatomically standardized MRI template. We designated this software program as the easy Z score imaging system (eZIS). Each SPECT image of one of the 31 healthy volunteers was also compared with the averaged SPECT image of the remaining 30 healthy volunteers in the same manner as in the patients. Using the averaged value of positive Z scores in already defined regions with a significant decline in rCBF in patients as the threshold, receiver operating characteristic (ROC) curves were determined using the ROCKIT 0.9β and the PlotROC programs developed by Metz et al. (http://xray.bsd.uchicago.edu/krl) [18]. The program calculates the area under the ROC curves (Az), accuracy, sensitivity, and specificity. The program also calculates statistical

significance for ROC curves using a partial area index [19]. Accuracy was determined as the value at the point where the sensitivity is the same as the specificity on the ROC curve.

Results

The SPM99 analysis demonstrated significant declines in adjusted rCBF of patients only in the posterior cingulate gyrus before (−8 −55 25, x y z; Z=5.22) and after (−10 −53 28, x y z; Z=5.49) PVC (Fig. 1) in the first group. This region with significant rCBF decline in the posterior cingulate gyrus is delineated as a specific region of interest for very early AD.

Then the averaged value of positive Z scores in this specific region was obtained in a Z score map before and after PVC (Fig. 2) in the second group. Using these averaged Z score values in the specific region of the posterior cingulate gyrus, the ROC curves for discrimination of patients from healthy volunteers were computed (Fig. 3). The PVC remarkably elevated *Az* and accuracy from 0.816 to 0.906 and from 73.9% to 83.7% respectively with global mean normalization. The PVC mildly elevated *Az* and accuracy from 0.811 to 0.832 and from 73.1% to 76.3% respectively with cerebellar normalization. There were significant differences in the partial area index for ROC curves between conditions with and without PVC after global mean normalization (two-tailed

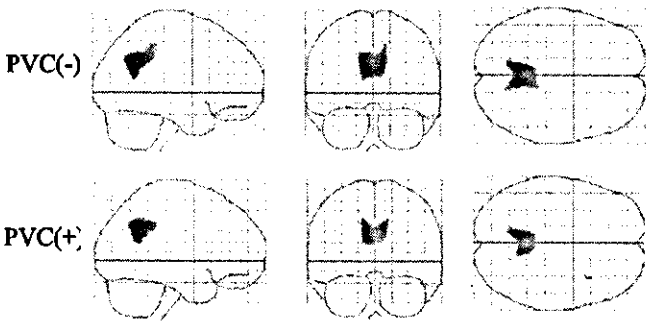

Fig. 1. Maximum intensity projections of SPM99 results for significant decline in adjusted rCBF in very early AD patients as compared with age-matched healthy volunteers before (*top*; −8 −55 25, x y z; Z=5.22; Brodmann area 31) and after (*bottom*; −10 −53 28, x y z; Z=5.49; Brodmann area 31) partial volume correction (*PVC*). Height threshold <0.001, corrected for multiple comparisons, extent threshold of 0 voxel

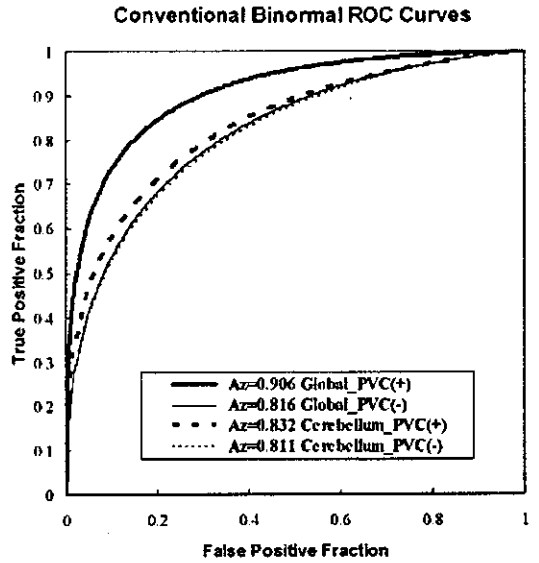

Fig. 3. ROC curves for discrimination between probable AD patients at the very early stage and healthy volunteers before and after PVC with voxel normalization to global mean (*thick solid line*, after PVC; *thin solid line*, before PVC) and cerebellar values (*thick dotted line*, after PVC; *thin dotted line* before PVC) when thresholding at the averaged values of positive Z scores in the posterior cingulate gyrus

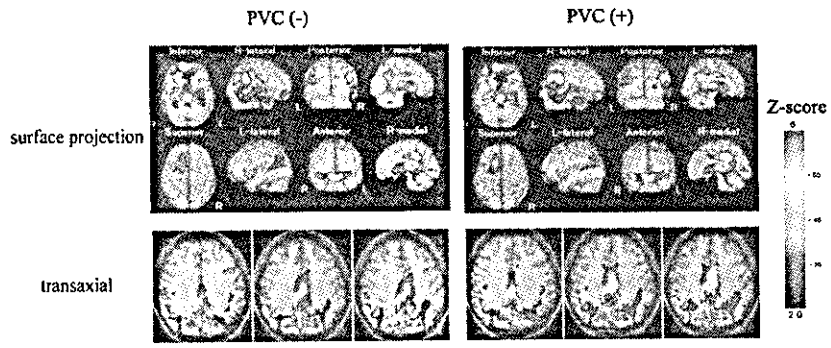

Fig. 2. Automated voxel-by-voxel Z score analysis by comparison of a SPECT image for a 75-year-old man with probable AD with an MMSE of 26 with the mean and standard deviation SPECT images of healthy volunteers after standardization to global mean voxel values. The Z score maps were displayed by overlaying on transaxial sections and surface projection of the spatially normalized MRI template. The PVC (*right*) showed a higher Z score than the uncorrected condition (*left*) in the posterior cingulate gyrus. *Red lines* enclose areas with a significant decline in adjusted rCBF in very early AD obtained from group comparison with healthy volunteers by SPM99

P value, 0.041), but no significant differences between conditions with and without PVC after cerebellar normalization (two-tailed *P* value, 0.5505).

Before PVC, SDs of control database in the posterior cingulate gyrus were 0.18 and 0.18 with global mean and cerebellar normalization respectively in the second group. After PVC, SDs of control database were 0.15 and 0.18 with global mean and cerebellar normalization respectively.

Discussion

In the present study, automated voxel-based analysis using a *Z* score value in the posterior cingulate gyrus after anatomical standardization of SPECT images revealed an accuracy of around 73% in discrimination of AD patients at the very early stage from healthy volunteers. The PVC elevated this accuracy to 83.7% with global mean normalization.

The rCBF or metabolic reduction in the posterior cingulate gyri and precunei has been established to characterize early to moderate AD even after PVC [6, 20]. Recent prospective studies on MCI patients reported that AD converters showed a significant metabolic reduction in the posterior cingulate gyrus and parietal association cortex as compared with AD nonconverters [21, 22]. The posterior cingulate gyrus has been reported to be much less atrophied than medial temporal structures in AD in spite of marked rCBF or metabolic decrease [23]. A slightly higher *Z* score value was obtained in the posterior cingulate gyrus after PVC than before PVC in the group comparison of patients and controls using SPM99. Although PVC has been reported to lessen the regional metabolic difference between patients with AD and control subjects [20], a 9.8% increase in accuracy was obtained after PVC with global mean normalization. This increase in the *Z* score value may have been due to a 17% reduction in the SD of the control database after PVC. It is very important in practice that three additional subjects, corresponding to 9.8% of 31 patients, were thereby correctly diagnosed.

Concerning the reference regions for voxel normalization, Soonawala et al. [24] reported that cerebellar normalization produced more accurate diagnostic results in single-scan SPM analysis of AD patients than did global mean normalization in ^{99m}Tc-hexamethylpropylene amine oxime SPECT. However, compared with the present investigation, they studied more advanced AD patients with an average MMSE score of 21.9. In the present study before PVC, global mean normalization provided almost equal accuracy to cerebellar normalization for discrimination of patients and controls. Improvement in accuracy after PVC was less pronounced with cerebellar normalization than with global mean normalization. This may have been due to the absence of a reduction in the SD of the control database after PVC with cerebellar normalization. Bartenstein et al. [25] used thalamic normalization in ^{99m}Tc-ECD SPECT. They considered global mean normalization to be inappropriate for a disease like AD with widespread metabolic or flow reduction and concluded that the thalamus is the most robust reference region for SPECT images. However, the thalamus is pathologically known to be involved from an early stage [26]. Moreover, Johnson et al. [27] revealed a decrease in rCBF in the anterior thalamus in subjects with very early AD. We considered that global mean normalization is sufficient for routine clinical diagnosis of very early AD.

A method for automated diagnosis of brain perfusion SPECT was developed in the present study. In this software program, voxel-based analysis was performed using a *Z* score map calculated from comparison of a patient's data with the control database in the same manner as in a three-dimensional stereotactic surface projection (3D-SSP) method [16]. Anatomical standardization of SPECT images into a stereotactic space was performed using SPM99. Therefore this program was made from the combination of 3D-SSP and SPM99. It has been reported that 3D-SSP with two-dimensional surface projection of cortical activities is less sensitive to artifacts derived from incomplete anatomical standardization of brain with localized cortical atrophy [28]. However, a 3D-SSP technique loses information on three-dimensional location, which SPECT images inherently possess. This program has also the advantage of capability of incorporation of SPM results into automated analysis of *Z* score values as a region of interest. A specific region of interest can be determined by group comparison of SPECT images for patients with a neuropsychiatric disease with those for healthy volunteers using SPM.

Herholz et al. [29] developed an original software program based on an automated voxel-based procedure after anatomical image standardization for discrimination between probable AD and controls using ^{18}F-fluorodeoxyglucose PET. They reported 84% sensitivity and 93% specificity for the detection of very mild probable AD with an MMSE of more than 24. Although the current study used a similar voxel-based procedure for detection of very mild probable AD, the accuracy did not exceed 80% before PVC. The present PVC in a SPECT study can afford an accuracy of 83.7% after global mean normalization, which is close to that in a PET study. From this point of view, it would be preferable to perform PVC in a SPECT study for early diagnosis of AD, thereby overcoming the drawback of greater susceptibility to partial volume effects due to the lower spatial resolution as compared with PET.

Conclusion

A voxel-based automated analysis of brain perfusion SPECT using a *Z* score map was applied to discrimina-

tion between probable AD patients at the very early stage and age-matched healthy volunteers. ROC analysis of the maximum Z score in the posterior cingulate gyrus as a specific area for the very early stage of probable AD determined by SPM99 demonstrated accuracies of 73.9% and 83.7% before and after PVC, respectively, with voxel normalization of global mean values. The PVC mildly enhanced the accuracy from 73.1% to 76.3% with cerebellar normalization. The PVC would thus be of benefit for the early diagnosis of AD in a SPECT study.

Acknowledgements. We are very thankful to Mr. Tsutomu Souma and Mr. Naoharu Takemura for assistance in developing software programs, the technical staff in our hospital for data acquisition of SPECT and MRI, and Mr. John Gelblum for his proofreading of this manuscript.

References

1. Minoshima S, Foster NL, Kuhl DE. Posterior cingulate cortex in Alzheimer's disease. Lancet 1994; 344:895.
2. Minoshima S, Giordani B, Berent S, Frey KA, Foster NL, Kuhl DE. Metabolic reduction in the posterior cingulate cortex in very early Alzheimer's disease. Ann Neurol 1997; 42: 85–94.
3. Kogure D, Matsuda H, Ohnishi T, Asada T, Uno M, Kunihiro T, Nakano S, Takasaki M. Longitudinal evaluation of early Alzheimer's disease using brain perfusion SPECT. J Nucl Med 2000; 41:1155–1162.
4. Okamura N, Arai H, Maruyama M, Higuchi M, Matsui T, Tanji H, Seki T, Hirai H, Chiba H, Itoh M, Sasaki H. Combined analysis of CSF tau levels and [^{123}I]iodoamphetamine SPECT in mild cognitive impairment: implications for a novel predictor of Alzheimer's disease. Am J Psychiatry 2002; 159: 474–476.
5. Matsuda H, Kanetaka H, Ohnishi T, Asada T, Imabayashi E, Nakano S, Kato A, Tanaka F. Brain SPET abnormalities in Alzheimer's disease before and after atrophy correction. Eur J Nucl Med Mol Imaging 2002; 29:1502–1505.
6. Sakamoto S, Matsuda H, Asada T, Ohnishi T, Nakano S, Kanetaka H, Takasaki Ml. Apolipoprotein E genotype and early Alzheimer's disease: a longitudinal SPECT study. J Neuroimaging 2003; 13:113–123.
7. Matsuda H, Ohnishi T, Asada T, Li ZJ, Kanetaka H, Imabayashi E, Tanaka F, Nakano S. Correction for partial-volume effects on brain perfusion SPECT in healthy men. J Nucl Med 2003;44:1243–1252.
8. McKhann G, Drachman D, Folstein M, Katzman R, Prie D, Stadlan EM. Clinical diagnosis of Alzheimer's disease: report of the NINCDS-ADRDA work group under the auspices of Department of Health and Human Service Task Force on Alzheimer's Disease. Neurology 1984; 34:939–944.
9. Petersen RC, Doody R, Kurz A, Mohs RC, Morris JC, Rabins PV, Ritchie K, Rossor M, Thal L, Winblad B. Current concepts in mild cognitive impairment. Arch Neurol 2001; 58: 1985–1992.
10. Hughes CP, Berg L, Danziger WL, Coben LA, Martin RL. A new clinical scale for the staging of dementia. Br J Psychiatry 1982; 140:566–572.
11. Folstein MF, Folstein SE, McHugh PR. Mini-Mental State: a practical method for grading the cognitive state of patients for the clinician. J Psychiatr Res 1975; 12:189–198.
12. Muller-Gartner HW, Links JM, Prince JL, Bryan RN, McVeigh E, Leal JP, Davatzikos C, Frost JJ. Measurement of radiotracer concentration in brain gray matter using positron emission tomography: MRI-based correction for partial volume effects. J Cereb Blood Flow Metab 1992; 12:571–583.
13. Labbe C, Froment JC, Kennedy A, Ashburner J, Cinotti L. Positron emission tomography metabolic data corrected for cortical atrophy using magnetic resonance imaging. Alzheimer Dis Assoc Disord 1996; 10:141–170.
14. Talairach J, Tourmoux P. Co-planar stereotaxic atlas of the human brain. New York: Thieme Medical, 1988.
15. Ohnishi T, Matsuda H, Hashimoto T, Kunihiro T, Nishikawa M, Uema T, Sasaki M. Abnormal regional cerebral blood flow in childhood autism. Brain 2000; 123:1838–1844.
16. Minoshima S, Frey KA, Koeppe RA, Foster NL, Kuhl DE. A diagnostic approach in Alzheimer's disease using three-dimensional stereotactic surface projections of fluorine-18-FDG PET. J Nucl Med 1995; 36:1238–1248.
17. Ishii K, Sasaki M, Matsui M, Sakamoto S, Yamaji S, Hayashi N, Mori T, Kitagaki H, Hirono N, Mori E. A diagnostic method for suspected Alzheimer's disease using $H_2{}^{15}O$ positron emission tomography perfusion Z score. Neuroradiology 2000; 42:787–794.
18. Metz CE, Herman BA, Roe CA. Statistical comparison of two ROC-curve estimates obtained from partially-paired datasets. Med Decis Making 1998; 18:110–121.
19. Jiang Y, Metz CE, Nishikawa RM. A receiver operating characteristic partial area index for highly sensitive diagnostic tests. Radiology 1996; 201:745–750.
20. Ibanez V, Pietrini P, Alexander GE, Furey ML, Teichberg D, Rajapakse JC, Rapoport SI, Schapiro MB, Horwitz B. Regional glucose metabolic abnormalities are not the result of atrophy in Alzheimer's disease. Neurology 1998; 50:1585–1593.
21. Chetelat G, Desgranges B, De La Sayette V, Viader F, Eustache F, Baron JC. Mild cognitive impairment: Can FDG-PET predict who is to rapidly convert to Alzheimer's disease? Neurology 2003; 60:1374–1377.
22. Berent S, Giordani B, Foster N, Minoshima S, Lajiness-O'Neill R, Koeppe R, Kuhl DE. Neuropsychological function and cerebral glucose utilization in isolated memory impairment and Alzheimer's disease. J Psychiatr Res 1999; 33:7–16.
23. Matsuda H, Kitayama N, Ohnishi T, Asada T, Nakano S, Sakamoto S, Imabayashi E, Katoh A. Longitudinal evaluation of both morphologic and functional changes in the same individuals with Alzheimer's disease. J Nucl Med 2002; 43:304–311.
24. Soonawala D, Amin T, Ebmeier KP, Steele JD, Dougall NJ, Best J, Migneco O, Nobili F, Scheidhauer K. Statistical parametric mapping of (^{99m})Tc-HMPAO-SPECT images for the diagnosis of Alzheimer's disease: normalizing to cerebellar tracer uptake. Neuroimage 2002; 17:1193–1202.
25. Bartenstein P, Minoshima S, Hirsch C, Buch K, Willoch F, Mosch D, Schad D, Schwaiger M, Kurz A. Quantitative assessment of cerebral blood flow in patients with Alzheimer's disease by SPECT. J Nucl Med 1997; 38:1095–1101.
26. Braak H, Braak E. Neuropathological staging of Alzheimer-related changes. Acta Neuropathol 1991; 82:239–256.

27. Johnson KA, Jones K, Holman BL, Becker JA, Spiers PA, Satlin A, Albert MS. Preclinical prediction of Alzheimer's disease using SPECT. Neurology 1998; 50:1563–1571.
28. Ishii K, Willoch F, Minoshima S, Drzezga A, Ficaro EP, Cross DJ, Kuhl DE, Schwaiger M. Statistical brain mapping of ^{18}F-FDG PET in Alzheimer's disease: validation of anatomic standardization for atrophied brains. J Nucl Med 2001; 42:548–557.
29. Herholz K, Salmon E, Perani D, Baron JC, Holthoff V, Frolich L, Schonknecht P, Ito K, Mielke R, Kalbe E, Zundorf G, Delbeuck X, Pelati O, Anchisi D, Fazio F, Kerrouche N, Desgranges B, Eustache F, Beuthien-Baumann B, Menzel C, Schroder J, Kato T, Arahata Y, Henze M, Heiss WD. Discrimination between Alzheimer dementia and controls by automated analysis of multicenter FDG PET. Neuroimage 2002; 17:302–316.

原著

軽度認知機能障害の脳血流および形態変化
—茨城県利根町における横断研究—

根本　清貴[1)3)], 山下　典生[2)], 大西　隆[3)], 今林　悦子[3)]
平尾健太郎[3)], 横銭　拓[2)], 佐々木恵美[2)], 水上　勝義[2)]
松田　博史[4)], 朝田　隆[2)]

抄　録

茨城県利根町において軽度認知機能障害を有する高齢者の脳機能・形態変化を神経画像検査により評価した．認知機能の評価を行い，65歳以上の1,711人から完全な神経心理検査の結果が得られた．記憶のみに障害を認め，それ以外は正常範囲のものを障害の程度に応じてPre-Dementia-1SD (PD-1SD), PD-1.5SDと分類した．PD-1SD 33人，PD-1.5SD 19人，ノーマル91人の計143人にMRIとSPECTを施行し，部分容積効果補正を行った後，SPM99を用いて灰白質の血流および容積を群間で比較した．脳血流ではPD-1SD, PD-1.5SDともに楔前部，右前頭前野での低下を認め，PD-1.5SDではさらに海馬傍回での低下を認めた．形態的にはPD-1.5SDで海馬傍回に萎縮を認め，PD-1.5SDがADの極早期の状態であると考えられた．さらにPD-1SDは，PD-1.5SDの先駆状態であることが示唆された．

Regional cerebral blood flow change and gray matter loss in mild cognitive impairment: a community-based study
Kiyotaka Nemoto[1)3)], Fumio Yamashita[2)], Takashi Ohnishi[3)], Etsuko Imabayashi[3)], Kentaro Hirao[3)], Hiromu Yokozeni[2)], Megumi Sasaki[2)], Katsuyoshi Mizukami[2)], Hiroshi Matsuda[4)], and Takashi Asada[2)]

[1)] 筑波大学附属病院精神神経科 [〒305-8576 茨城県つくば市天久保2-1-1]
[2)] 筑波大学臨床医学系精神医学 [〒305-8577 茨城県つくば市天王台1-1-1]
[3)] 国立精神・神経センター武蔵病院放射線診療部 [〒187-8551 東京都小平市小川東町4-1-1]
[4)] 埼玉医科大学国際医療センター核医学 [〒350-0495 埼玉県入間郡毛呂山町毛呂本郷38]

はじめに

軽度認知機能障害 (Mild Cognitive Impairment: MCI) とは，健常人に比し認知機能が障害されてはいるが，アルツハイマー病 (AD) などの痴呆には至っていない状態として受け入れられつつある．しかし，今のところMCIの確立した診断基準はなく，研究者により様々に異なる．代表的な基準はPetersenらによるものであり，その骨格は主観・客観的に選択的な記憶障害を認める点にある．これまで健常者におけるアルツハイマー病の発症率は年1-2%とされてきたが，彼らのいうMCI群では年10-15%と報告されている (Petersen et al., 1999)．しかし，このMCIの診断基準には多くの疑問が投げかけられている．Petersen自身が近年，

MCIをさらにamnestic MCI, multiple-domain MCI, single non-memory-domain MCIとする亜分類を試みている（Petersen et al., 2001）が，今のところ統一見解は示されていない．

Petersenらの診断基準の他に，国際老年精神医学会では，“Ageing-Associated Cognitive Decline”（AACD）という概念を提唱している（Levy, 1994）．このAACDの診断基準の特徴は，標準化された神経心理学検査において記憶，注意，思考，言語，視空間認知のいずれかの機能が，年齢，性別，教育歴を考慮したうえで健常人に比し1SD以上低い点にある．つまりその特徴は，記憶に限定せず，複数の認知機能に注目していることである．このAACDの診断基準の方が臨床上の有用性においてMCIの診断基準に優るとする報告もある（Ritchie et al., 2001）が，今のところMCI, AACDのいずれについても大規模な疫学調査や予後に関する研究は限られている．

近年，画像統計解析手法の発展により，軽度認知機能障害または早期アルツハイマー病（AD）におけるPET, SPECTでの報告が数多く見られるようになってきた（Minoshima et al., 1997, Kogure et al., 2000, Wolf et al., 2003, Huang et al., 2002）．これらの報告に共通して見られる所見は，MCIの時点において帯状回後部もしくは楔前部に血流低下や糖代謝低下が認められることである．

しかし，これらの研究の対象者は原則として病院を受診した個人であり，大規模な疫学調査における軽度認知機能障害群の脳機能画像所見は現在まで報告されていない．そこで，我々は2001年11月より3年間にわたって，茨城県利根町に住む65歳以上の住民を対象とした前向きコホート研究を継続した．そこでは，神経心理検査及び画像検査を用いて軽度認知機能障害群の予後を追跡した．本稿では研究開始時に認知機能障害を呈していると診断された個人における脳機能画像所見を報告する．

対象と方法

略述すると，茨城と千葉の県境に位置する茨城県利根町に住む65歳以上の全住民2,949人に研究への参加を呼びかけた．その結果，71%の参加可能な町民が研究に同意し，書面によるインフォームドコンセントが得られた．またフルデータが得られた者は1,711名であった．本研究は筑波大学医の倫理委員会にて承認されている．

神経心理学的方法

まず，神経心理学的スクリーニングとして，痴呆前駆状態診断の目的に特化した集団スクリーニングテスト，「ファイブコグ」を施行した．このテストは最大50人までの集団で同時に施行可能であり，我々が東京都老人総合研究所精神医学部門と共同開発をしたものである．ファイブコグはAACDの概念にならって認知機能のうち，記憶，注意，言語，視空間認知，類推に着目した設問から構成されている．ファイブコグの個々の設問は表面妥当性はあると考えられた以下の検査から採っている．記憶は手がかり再生 Category cued recall (Grober et al., 1988)，注意は位置判断 Set dependency activity (Sohlberg and Mateer, 1986)，言語では動物名想起 Category verbal fluency (Monsch et al., 1992)，視空間認知は時計描画 Clock drawing test (Mendez, 2000)，そして類推はWAIS-Rの下位項目の類推（Wechsler, 1981）である．

このファイブコグのテスト再テスト信頼性を確認するために，38名の対象者において平均64日間の間隔で2回検査を施行した．そして5つの設問それぞれについて相関係数とp値を算出した．その結果，いずれについても$p<0.0001$であり，これによりテスト再テスト信頼性があると考えられた．被検者全員にこのバッテリー